SUPPORTING INFORMATION

Label-free probing electron transfer kinetics of single microbial cells on a single-layer graphene via structural color microscopy

Qing Xia[a], Xueqin Chen[a], Changhong Liu[b], Rong-Bin Song[a], Zixuan Chen[a,*], Jianrong Zhang [a,*] and Jun-Jie Zhu[a,*]

[a] School of Chemistry and Chemical Engineering, Nanjing University, 163 Xianlin Ave, Nanjing 210023, PR China

[b] The State Key Laboratory of Pharmaceutical Biotechnology, School of Life Science, Nanjing University, Nanjing 210023, P. R. China

Email: chenzixuan@nju.edu.cn, jrzhang@nju.edu.cn, jjzhu@nju.edu.cn

Experimental Details

1. Chemicals and general technologies.

S. oneidensis MR-1 and *E. coli* were purchased from American Type Culture Collection (Manassas, VA, USA). *P. aeruginosa* (CGMCC 1.512) was purchased from China General Microbiological Culture Collection Center, Institute of Microbiology Chinese Academy of Sciences (Beijing, China). Luria-Bertani (LB) broth and Na_2S were purchased from Sigma-Aldrich (Shanghai, China). 2.5% glutaraldehyde was diluted from 25% glutaraldehyde, which was purchased from Sinopharm Reagent (Beijing, China). Ultrapure water with a resistivity of 18.2 MΩ cm was produced using a Milli-Q apparatus (Millipore) and used in the preparation of all solutions. Cover slides were purchased from Thorlabs Co., Ltd. PDMS was prepared using Sylgard 184, Dow Corning. All media and solutions were sterilized before use.

Scanning electron microscopy (SEM) images were collected on a JEOL JSM-7800F scanning electron microscope (Hitachi Co., Japan). Absorbance scans were performed on an Agilent Cary 5000 UV-Vis-NIR spectrophotometer. Dark-field images and spectra measurements were carried out on Nikon Ti-E microscope. A broadband light source (EQ-99XFC LDLS, Energetiq Technology) was used for incident illumination. True-color dark-field images are captured by a color cooled digital camera (DS-RI1, Nikon), and the scattering spectra of single bacteria was measured by a monochromator (Acton SP2300i, PI) equipped with a spectrograph CCD (PIXIS 400BR_excelon, PI) and a grating (grating density: 300 L mm^{-1}; blazed wavelength: 500 nm).

2. Cell culture.

S. oneidensis MR-1, *E. coli*, *P. aeruginosa* were cultured in 50 ml centrifuge tube containing of 15 mL LB broth medium at 30 ℃ overnight on a shaker (150 rpm). For anaerobic culture, N_2 was introduced into the LB broth medium for 30 minutes to completely remove O_2 and the bottle cap was tightened to be sealed. The bacterial cells were harvested by centrifugation (5000 rpm, 5 min) and dispersed in ultrapure water for further use.

3. SEM analysis.

S. oneidensis MR-1 cells were suspended in a 2.5% glutaraldehyde solution over 1 h for cell fixation, and then dehydrated in increasing concentrations of ethanol solution (25%, 50%, 75%, 85%, 95%, and 100%). Finally, Indium tin oxide glass was dipped into the ethanol solution of *S. oneidensis* MR-1 cells, and dried under ambient conditions for SEM tests.

4. UV-visible spectroscopy of *S. oneidensis MR-1*.

The aerobic cultured *S. oneidensis* MR-1 were harvested by centrifugation (5000 rpm, 5 min) and suspended in 5 mL PBS (pH = 7.4) buffer before aliquots were transferred to 1 cm pathlength quartz cuvettes. 50 μM Na_2S was dissolved in PBS (pH = 7.4) buffer to produce 50 μM H_2S into the environment. Na_2S was added into the cells to 25 μM final concentration. Absorbance scans were performed on an Agilent Cary 5000 UV-Vis-NIR spectrophotometer.

5. Oxygen and Hydrogen Sulfide Treatment.

Blow O_2 into the solution for 10 min to make O_2 sufficient (concentration > 19.99 mg/L). 50 μM Na_2S was dissolved in PBS (pH = 7.4) buffer to produce 50 μM H_2S into the environment. The solution was flowed in and out with two injectors.

6. Measuring the quantum efficiency of color cooled digital camera.

In order to measure the quantum efficiency of the color cooled digital camera (DS-RI1, Nikon), we installed bandpass filters (FKB-VIS-10, Thorlabs Co., Ltd) of wavelengths from 400 nm to 800 nm on the optical path of the

broadband light source (EQ-99XFC LDLS, Energetiq Technology). True-color images were captured at different wavelengths. We split the true-color images into RGB channels, and obtain the quantum efficiency by analyzing the light intensity at different wavelengths in RGB channels.

7. Fabrication of the electrochemical cell.

The transparent single-layer graphene electrode used in this work was constructed according to the method reported in our previous work [1]. A 47-nm-thick gold film was coated on a cover slide, followed by treatment of gold etchant for 1 min in the center. The remaining gold film was used for connection between the graphene and the potentiostat. A CVD graphene sample was transferred onto the etched hole of the gold substrate with a PMMA-mediated approach. Simply, a layer of PMMA was spin-coated onto the graphene, and the metal below it was etched away completely. The PMMA/graphene stack was then transferred onto the Au surface. After the graphene was transferred onto the gold substrate, the PMMA layer was dissolved and removed by acetone. An electrochemical cell (with 3 mm inner diameter) made of PDMS was placed on top of the graphene sample, and M9 buffer solution was used as electrolyte. The potential of graphene was controlled with respect to Ag/AgCl reference electrode with the potentiostat using a platinum wire as counter electrode.

8. Simultaneous Electrochemical and Scattering Measurements.

The electrochemical cell was placed on the 100× oil immersion objective (NA=1.49) equipped by a Nikon Ti-E inverted microscope. N_2 flow into the electrochemical cell was started just before the beginning of the measurements. Scattering imaging and electrochemical measurements were started simultaneously. In cyclic voltammetry measurements, the working electrode potential was swept at 1 mV/s from -0.2 V to 0.6 V, while scattering images were acquired in the interval of 10 s.

9. Theoretical simulations.

For simulating scattering spectra of single *S. oneidensis* MR-1, three-dimensional FDTD simulations from Lumerical Solutions, Inc. (Vancouver, Canada) were performed. We constructed a multi-layer core-shell rod-like model [2-4] consists of cytoplasm, inner membrane (IM), periplasm, OM and cytochrome layer. We chose periplasmic decaheme cytochrome MtrA, transmembrane porin MtrB and OM decaheme cytochrome MtrC as a representative. The model is 1.5 μm in length and 0.4 μm in diameter, which were the mean sizes of *S. oneidensis* MR-1 (Fig. S2). The thickness of IM and periplasm are 5 nm and 23.5 nm [4, 5]. The thickness of the OM cytochromes layer, the periplasmic cytochromes layer and the transmembrane cytochromes layer is 6.5 nm, 5 nm and 10 nm, respectively [3, 4]. The average refractive index of oxidized, reduced cytochromes, periplasm and cytoplasm are 1.844 [6], 2.168 [6], 1.500 [7] and 1.360 [8], respectively. The maximum refractive index of oxidized cytochromes is 2.098 [6]. The minimum and maximum refractive index of reduced cytochromes is 1.924 and 2.387 [6]. So, the average refractive index of oxidized and reduced OM cytochromes layer is 1.844 and 2.168, due to the tightly packed MtrC in OM [4]. The average refractive index of oxidized and reduced MtrA and MtrB layer are 1.672 and 1.834, due to the about 50 % density in OM and periplasm [4]. A plane wave source served as the incident light in the simulation region. The boundary conditions of the simulation domain are perfectly matched layer (PML). The calculation region was 5×5×10 μm^3, in which the grid resolution was set to 0.01 μm. The refractive index of the surrounding medium was set to be 1.33 for water.

10. Quantitatively measurement of ET dynamics.

To directly characterize the electrons transport, we linked the scattering color of *S. oneidensis* MR-1 to the cytochrome redox state. Through fitting and calculation, we converted the change of scattering color to the number of transferred electrons during one electron transfer process.

Initially, we calculated the number of cytochromes in single *S. oneidensis* MR-1. In this work, we simplified one *S. oneidensis* MR-1 to a rod-like model. The maximum number of MtrC on a cell surface can be approximately calculated with the projected area of one MtrC and the sum of external surface area of a cell, S_{MtrC} and S_{cell}, and given by

$$N_{MtrC} = \frac{S_{cell}}{S_{MtrC}} \qquad \text{(S1)}$$

where $S_{MtrC} = \pi r^2$, and r is the radius of MtrC, found to be 4.75 nm[3], $S_{cell} = S_1 + S_2$. S_{cell} can be divided into the external surface area of both ends of cell (S_1), considered as two hemispheres, and external surface area of cell body (S_2), considered as a cylinder.

According to the formula for the surface area of spheres and cylinders, we have $S_1 = 4\pi\,(L_1/2)^2$ and $S_2 = \pi L_1 \times (L - L_1)$, L_1 and L is the diameter and length of one *S. oneidensis* MR-1 cell, which are shown in Fig. S13. According to eq (S1), N_{MtrC} is calculated to be $4.43 \times 10^{16} L L_1$. There are ten cytochromes in a single decaheme cytochrome MtrC, thus he maximum number of cytochromes on the surface of a single cell N_{Cyt} is calculated to be $4.43 \times 10^{17} L L_1$.

Assuming that *C* is the coverage of cytochromes on the surface of a single bacterium, with a fixed value between 0 and 1, and f_{red} is the content of reduced cytochromes on the surface of a single bacterium, the real-time refractive index of a single bacterium *n* is,

$$n = C f_{red} n_{red} + C(1 - f_{red}) n_{ox} + (1 - C) n_0 \qquad \text{(S2)}$$

where n_{red}, n_{ox} and n_0 are the refractive index of reduced, oxidized cytochromes and periplasm, found to be 1.844, 2.168[6] and 1.500[7], respectively.

The real-time electron number of a single bacterium N_e is determined by the number of cytochromes in the reduced state (+2) and oxidized (+3),

$$N_e = 2 f_{red} N_{Cyt\,c} C + 3(1 - f_{red}) N_{Cyt\,c} C \qquad \text{(S3).}$$

According to Fig. 4B, we have the correlation of calculated ratio of R/G and refractive index n,

$$R/G = 4.75 - 1.7n \qquad \text{(S4).}$$

Combining eqs (S2-S4),

$$N_e = \alpha\, R/G + \beta \qquad \text{(S5)}$$

where $\alpha = 0.59 N_{Cyt}/(n_{red} - n_{ox})$, $\beta = 3C N_{Cyt\,c} + N_{Cyt}\,[(1 - C)n_0 + C n_{ox} - 2.79]/(n_{red} - n_{ox})$. When cytochromes changed from reduced to oxidized, or from oxidized to reduced, we can obtain the number of electrons transferred by an individual cell ΔN_e according to eq (S5),

$$\Delta N_e = \alpha\, \Delta R/G \qquad \text{(S6).}$$

Simplifying eq (S6), we have the density of ET number Δn_e,

$$\Delta n_e = {\alpha\, \Delta R/G}\big/{S_{cell}} = \gamma \Delta\, R/G \qquad \text{(S7)}$$

where γ is expressed as $0.59 D_{Cyt}/(n_{red} - n_{ox})$, where D_{Cyt} is the density of cytochromes in OM, which is calculated to be 1.41×10^5 μm^{-2}, and γ is calculated to be 2.57×10^5 μm^{-2}. That is to say, the number of electrons transferred by an individual bacterium per square micron could be measured with the scattering color of the cell in this model.

Supporting Figures and Videos

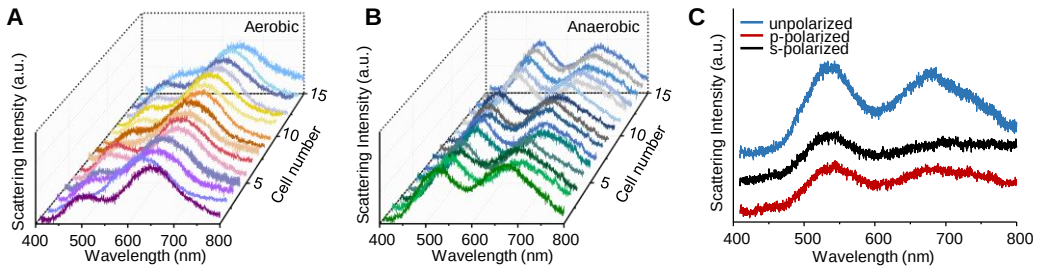

Figure S1. Measurement of scattering spectra of individual bacteria. (A-B) Scattering spectra of 15 random individual MR-1 cells cultured in aerobic (A) and (B) anaerobic conditions, related to Figure 2C-D. (C) Scattering spectra of an individual MR-1 cell under p- (red), s- (black) and unpolarized (blue) incident illumination.

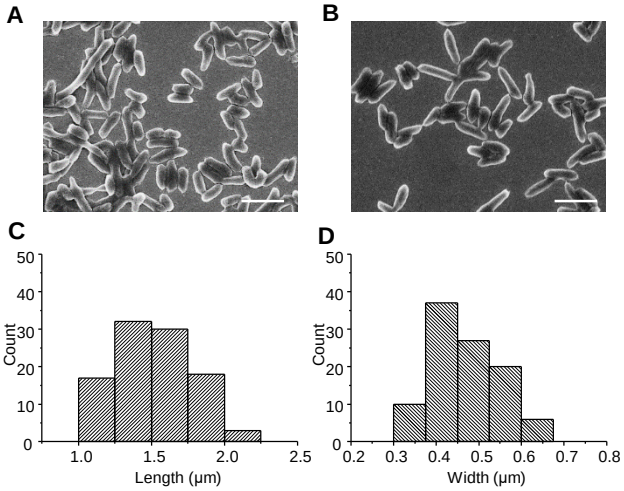

Figure S2. SEM characterization of *S. oneidensis* MR-1. (A, B) SEM image. Scale bar is 2 μm. (C, D) Histogram distributions of the length (C) and width (D) of 100 random cells, related to Figure 3A.

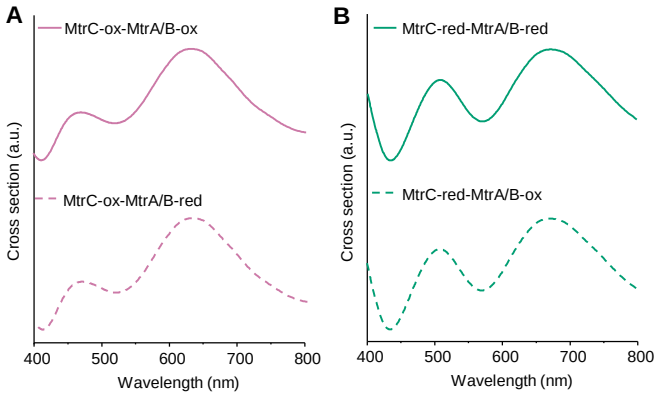

Figure S3. Calculated scattering cross-section of individual *S. oneidensis* MR-1 with different redox states of cytochromes. (A) MtrC is set to be oxidized, while MtrA and MtrB are set to be oxidized (solid line) and reduced (dash line). (B) MtrC is set to be reduced, while MtrA and MtrB are set to be oxidized (dash line) and reduced (solid line), related to Figure 3A.

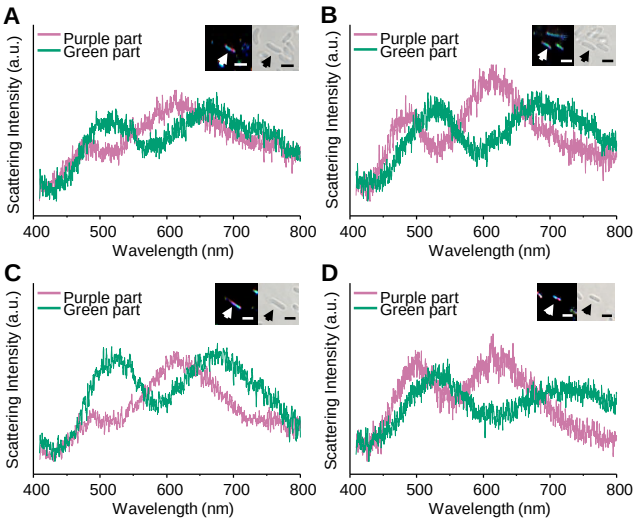

Figure S4. Inhomogeneous subcellular scattering spectra in individual *S. oneidensis* MR-1. (A-D) Scattering spectra of 4 individual cells with different colors. Insets are corresponding scattering and transmitted images. Scale bar is 1 μm, related to Figure 3F.

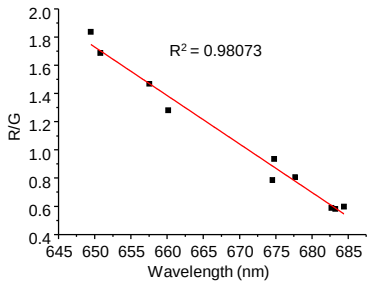

Figure S5. Correlation between the ratio of R- and G-channels of the color image and peak-α wavelength of individual *S. oneidensis* MR-1 cells.

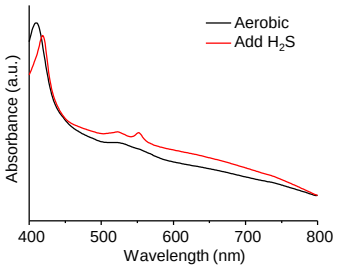

Figure S6. UV-visible Spectra of aerobic cultured *S. oneidensis* MR-1 before (black curve) and after (red curve) the addition of 50 μM H_2S, related to Figure 4.

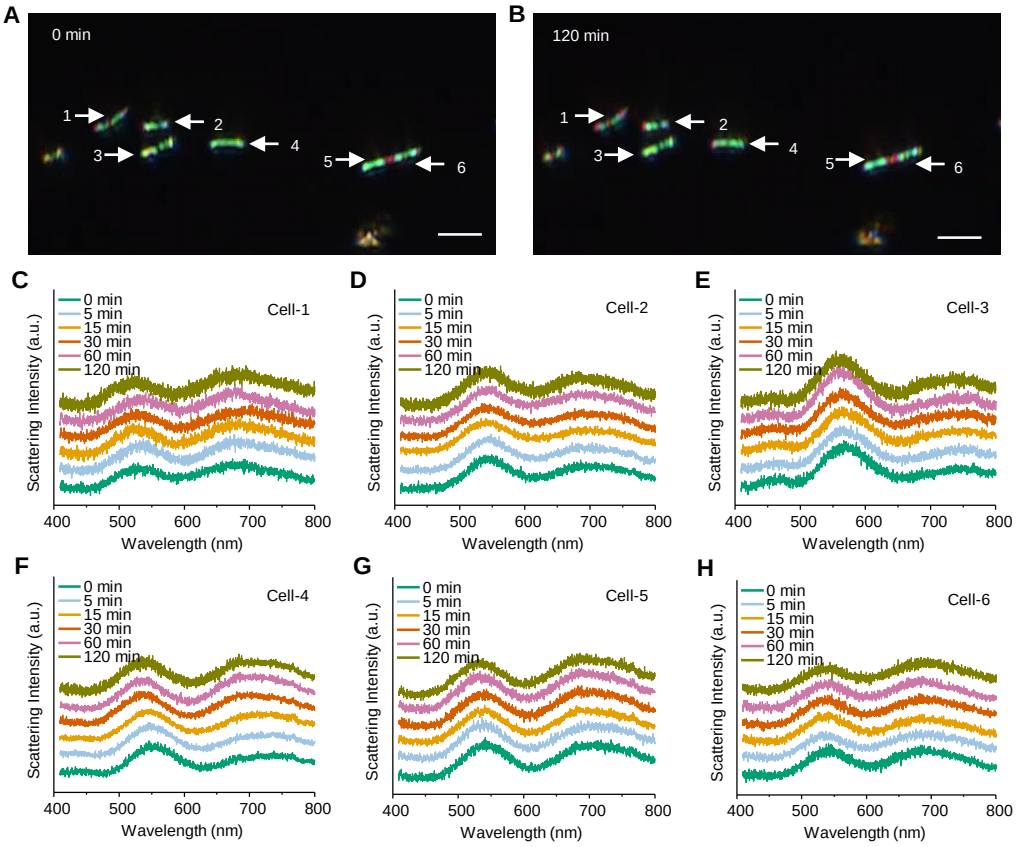

Figure S7. Measurement of electron transfer in anaerobic cultured *S. oneidensis* MR-1 without O_2 treatment. (A, B) Scattering image of anaerobic cultured cells in water before (A) and after (B) 120 min observation without O_2 treatment. Scale bar is 2 μm. (C-H) Scattering spectra of 6 labeled cells in (A) during the process, related to Figure 4.

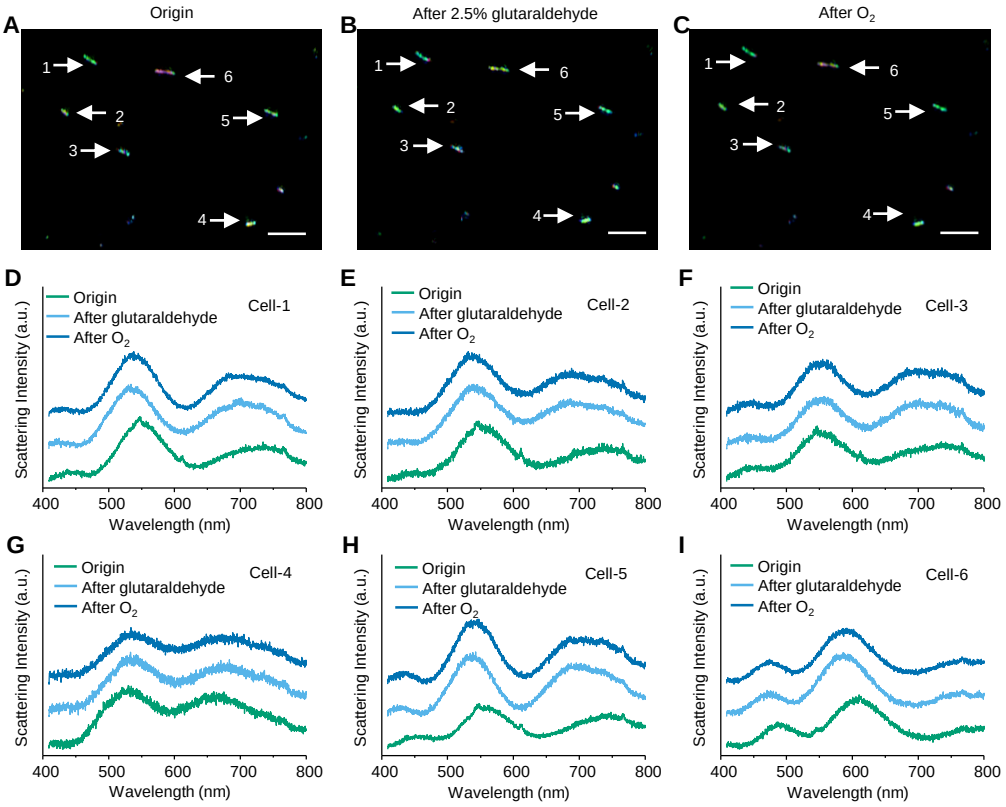

Figure S8. Measurement of electron transfer in inactivated *S. oneidensis* MR-1. (A) Scattering image of live cells. (B) Scattering image of cells immersed in 2.5% glutaraldehyde for 1 h. (C) Scattering image of cells in (B) with further treatment by O_2 for 1 h. Scale bar is 5 μm. (D-I) Scattering spectra of 6 labeled cells in (A-C) during the process, related to Figure 4.

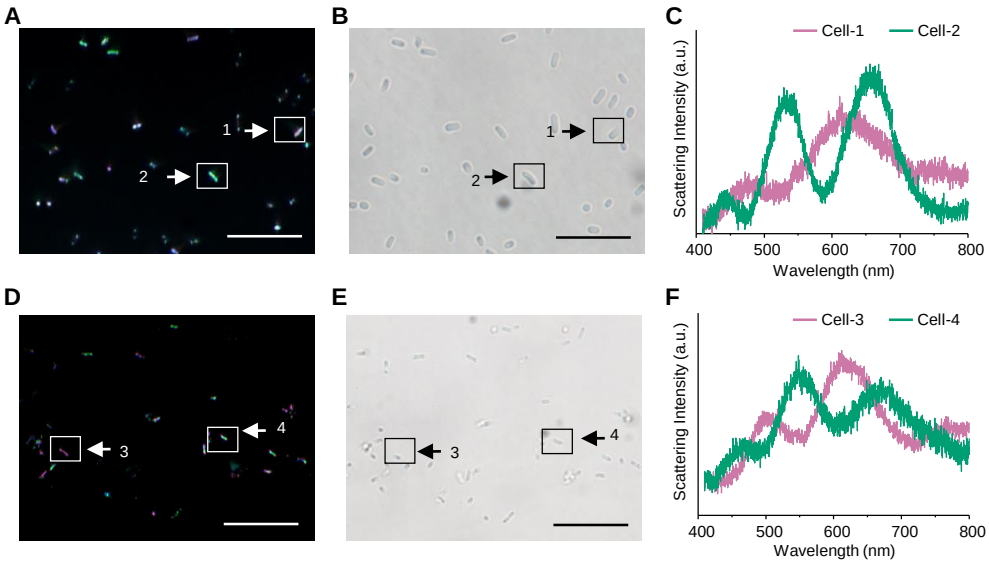

Figure S9. Observation of the elastic scattering from other Gram-negative bacteria. (A, B) Scattering (A) and transmitted (B) images of individual *P. aeruginosa* cells. Scale bar is 10 μm. (C) Scattering spectra of 2 labeled cells in (A). (D, E) Scattering (D) and transmitted (E) images of individual *E. coli* cells. Scale bar is 10 μm. (F) Scattering spectra of 2 labeled cells in (D).

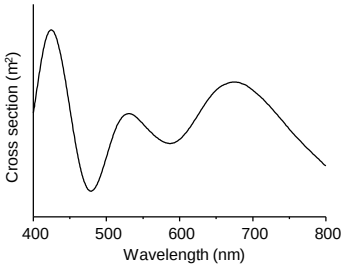

Figure S10. Calculated scattering cross-section of single *E. Coli* model with reduced OM cytochromes. The length of the model is 1.5 μm and the width is 0.44 μm.

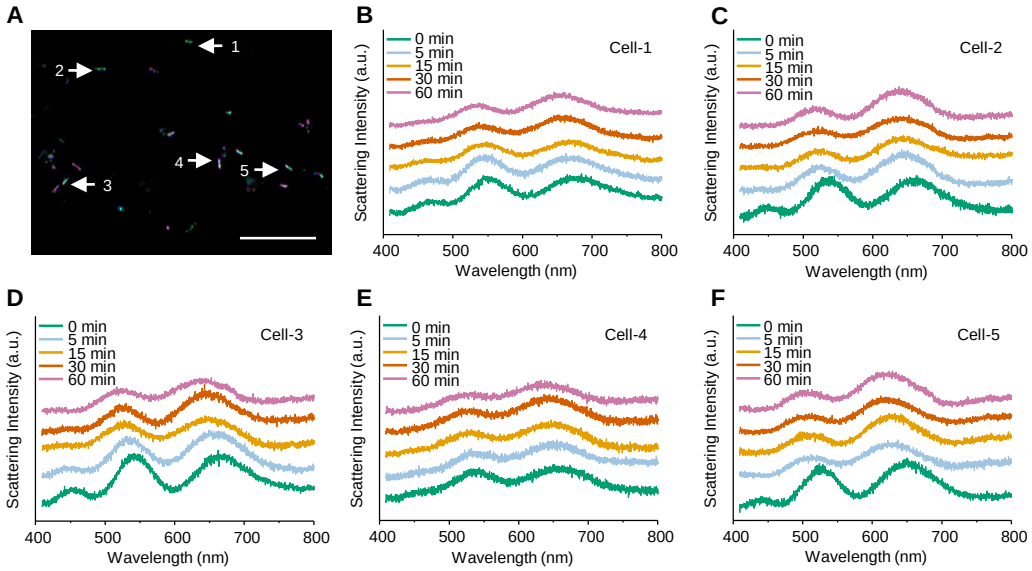

Figure S11. Redox state-responsive scattering of individual *E. Coli* cells. (A) Scattering image of *E. coli* cells. Scale bar is 10 μm. (B-F) Scattering spectra of 5 labeled cells in (A) with O_2 treatment for 0 to 60 min.

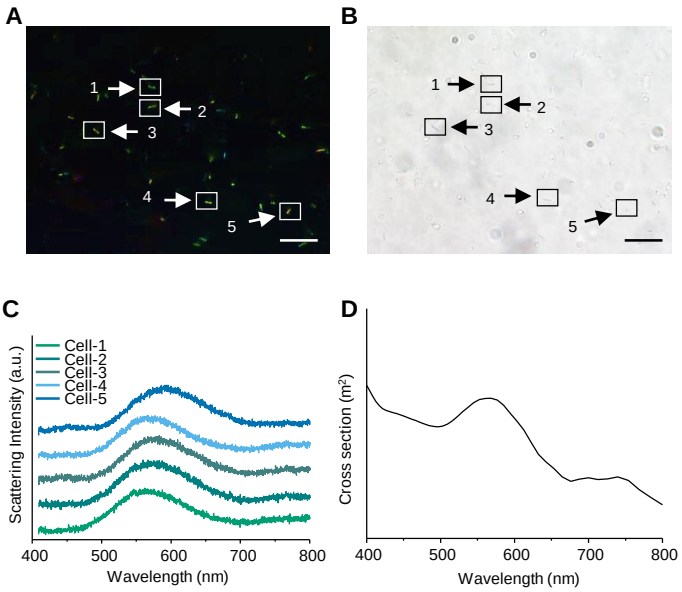

Figure S12. (A) Scattering image and (B) bright field image of *B. pumilus* under normal culture conditions. Scale bar is 10 μm. (C) Scattering spectra of cell 1-5 with boxes in (A-B). (D) Calculated scattering cross-section of *B. pumilus*. The total thickness of cell wall, periplasm and IM is set to 80 nm, and average refractive is set to 1.56.

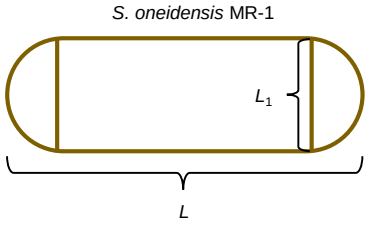

Figure S13. Simplified schematic planar structure of *S. oneidensis* MR-1.

Video S1. Video demonstrating the time-dependent subcellular scattering of an individual *S. oneidensis* MR-1 cell cultured in LB with limited O_2 for 30 min. Scale bar is 1 μm.

Video S2. Video demonstrating *R/G* value image sequence of multiple *S. oneidensis* MR-1 cells at different potentials during continuous cycling of the potential between -0.2 V to 0.6 V at a rate of 1 mV s^{-1}.

Video S3. Video demonstrating the time-dependent subcellular scattering of individual *S. oneidensis* MR-1 cells exposed to extra UV light (λ < 400 nm) for 90 min. Scale bar is 5 μm.

REFERENCE

1. Xia, Q.; Chen, Z.; Xiao, P.; Wang, M.; Chen, X.; Zhang, J.-R.; Chen, H.-Y.; Zhu, J.-J., Fermi level-tuned optics of graphene for attocoulomb-scale quantification of electron transfer at single gold nanoparticles. *Nat. Commun.* **2019,** *10* (1), 3849.

2. Breuer, M.; Rosso, K. M.; Blumberger, J.; Butt, J. N., Multi-haem cytochromes in Shewanella oneidensis MR-1: structures, functions and opportunities. *J. R. Soc. Interface* **2015,** *12* (102), 20141117.

3. Jiang, X.; Burger, B.; Gajdos, F.; Bortolotti, C.; Futera, Z.; Breuer, M.; Blumberger, J., Kinetics of trifurcated electron flow in the decaheme bacterial proteins MtrC and MtrF. *Proc. Natl. Acad. Sci.* **2019,** *116* (9), 3425.

4. Subramanian, P.; Pirbadian, S.; El-Naggar, M. Y.; Jensen, G. J., Ultrastructure of Shewanella oneidensis MR-1 nanowires revealed by electron cryotomography. *Proc. Natl. Acad. Sci.* **2018,** *115* (14), E3246-E3255.

5. Dohnalkova, A. C.; Marshall, M. J.; Arey, B. W.; Williams, K. H.; Buck, E. C.; Fredrickson, J. K., Imaging Hydrated Microbial Extracellular Polymers: Comparative Analysis by Electron Microscopy. *Applied and Environmental Microbiology* **2011,** *77* (4), 1254.

6. Simonson, T.; Perahia, D., Internal and interfacial dielectric properties of cytochrome c from molecular dynamics in aqueous solution. *Proc. Natl. Acad. Sci.* **1995,** *92* (4), 1082.

7. Spencelayh, M. J.; Cheng, Y.; Bushby, R. J.; Bugg, T. D. H.; Li, J.-j.; Henderson, P. J. F.; O'Reilly, J.; Evans, S. D., Antibiotic Action and Peptidoglycan Formation on Tethered Lipid Bilayer Membranes. *Angew. Chem. Int. Ed.* **2006,** *45* (13), 2111-2116.

8. Stoyan, T.; Valery, V. T.; Paul, P., Cell membrane and gold nanoparticles effects on optical immersion experiments with noncancerous and cancerous cells: finite-difference time-domain modeling. *Journal of Biomedical Optics* **2006,** *11* (6), 1-6.